A Dimensionality Reduction Approach in Helicopter Hover Performance Flight Testing

Arush, Ilan; Pavel, Marilena D.; Mulder, Max

DOI
10.4050/JAHS.67.032010

Publication date
2022

Document Version
Final published version

Published in
Journal of the American Helicopter Society

A Dimensionality Reduction Approach in Helicopter Hover Performance Flight Testing

Ilan Arush*
Chief of RW Performance & Flying Qualities Academics
National Test Pilot School, Mojave, CA

Marilena D. Pavel
Associate Professor

Max Mulder
Head of Control & Simulation
Faculty of Aerospace Engineering, Delft University of Technology
Delft, The Netherlands

The power required to hover a helicopter is fundamental to any new or modified performance flight-testing effort. The conventional method of relating two nondimensional variables (coefficients of power and weight) is overly simplified and neglects compressibility effects in the power required to hover under a wide range of gross weights and atmospheric conditions. An alternative flight-test method for assessing hover performance while addressing this deficiency of the conventional method is proposed. The method uses an original list of 15 corrected variables derived from fundamental dimensional analysis, which is further reduced by means of dimensionality reduction to include only the most essential and effective predictors. The method is demonstrated using data of a Bell Jet-Ranger and shows that at the 95% confidence level; the averaged prediction error is only 0.9 hp (0.3% of the maximum continuous power). Using the same data, the conventional method yields a much larger averaged prediction error of 1.7 hp.

Nomenclature

A_d	main rotor disk area, m^2
b	number of blades
$\vec{b}$	column vector, measured power to hover, hp
$\bar{C}$	average chord (main rotor blades), m
C_{d0}	zero-lift drag coefficient (main rotor blades)
$C_P = \frac{P}{\rho A_d (\omega R)^3}$	coefficient of power (entire helicopter)
$C_{P_{M/R}} = \frac{P_{M/R}}{\rho A_d (\omega R)^3}$	coefficient of power (main rotor only)
$C_W = \frac{W}{\rho A_d (\omega R)^2}$	coefficient of weight
$\vec{E}_r\|_i$	power prediction error vector for model (i), hp
$M_{tip} = \frac{\omega R}{\sqrt{\gamma R_{air} T_a}}$	tip Mach number (main rotor blades)
P	power required to hover (entire helicopter), hp
$P_{M/R}$	power required to hover (main rotor only), hp
P_a	ambient air static pressure, pa
P_o	standard sea level static air pressure (101325 pa), pa
R	main rotor disk radius, m
R_{air}	air gas constant (= 287), J/(kg·K)
S_i	standard deviation of prediction errors, model (i), hp
T_a	ambient air static temperature, K
T_0	standard sea-level static air temperature (288.15), K
t_i	test statistics for the prediction errors of model (i)
U	left singular vectors matrix of Z
V	right singular vectors matrix of Z
W	helicopter total gross weight, N, lb
Z	normalized corrected variables matrix
α, β	generic polynomial coefficients vector
γ	heat capacity ratio for air (1.4)
$\delta = P_a/P_o$	ambient air pressure ratio
$\theta = T_a/T_o$	ambient air temperature ratio
μ_i	mean value of prediction errors, model (i), hp
π_i	generic nondimensional variable
π_i^*	generic corrected variable (ND for a specific helicopter type)
ρ_a	ambient air density, kg/m^3
Σ	singular values matrix of Z
σ_i	singular values of matrix Z (elements along the diagonal of Σ)
$\sigma_R = \frac{b\bar{c}}{\pi R}$	main-rotor solidity ratio
ω	main-rotor angular speed, rad/s

Subscripts

i,j	indices
j	model number index

*Corresponding author; email: iarush@ntps.edu.
Manuscript received July 2021; accepted February 2022.

Introduction

The most distinguishing characteristic of a helicopter is its ability to steadily hover at any phase of its mission given it has a sufficient power margin (Refs. 1,2). Knowing the power required to hover is fundamental to any new or modified helicopter flight-test effort. The conventional flight-test method for hover performance is based on the combined blade-element momentum theory and is overly simplified. This simplification often yields empirical models that fail to accurately and consistently predict the total power required to hover

under a wide range of helicopter gross weight and atmospheric conditions. Bousman (Ref. 3) demonstrates this drawback by using out-of-ground effect (OGE) hover performance testing of five different flight-test programs and reporting inconsistency in OGE hover performance of up to 5% of which the source of the error could not be explained.

A major disadvantage of the conventional OGE hover flight-test method is that it does not address main rotor blade compressibility effects as those are often assumed to have a negligible effect on the hover performance. An example of this frequently taken assumption can be found in the study on uncertainty quantification in helicopter performance by Siva et al. (Ref. 4). The ability to account for compressibility effects, mostly related to blade tip Mach number and shape, is essential for accurate hover performance predictions. This relation is well illustrated by computational fluid dynamic (CFD) simulations used to predict the hover performance of rotor systems. Jacobson and Smith (Ref. 5) present a hover performance comparison between predictions from a hybrid CFD methodology and measured hover performance of a rotor with three different blade tip configurations at three different tip Mach numbers (0.55, 0.6, and 0.65). They state that future work is needed to understand why CFD models do not predict the same impact of the tip shape as measured in the experiment. Moreover, one of Ref. 5 conclusions states that hover performance predictions from the hybrid methodology CFD improve as tip Mach numbers reduce. This conclusion solidifies the significance compressibility effects have on hover performance. Garcia and Barakos (Ref. 6) provide another example to show compressibility effects should not be neglected from hover performance predictions. Their work, which focused on accurate rotor hover performance predictions using modern CFD methods with modest computer resources, shows the significance the tip shape and Mach number have on the hover performance of a rotor system.

Measuring compressibility effects in flight-testing of a full-scale helicopter and not just a rotor system requires the hover trials to be performed in high altitude and low air temperatures. Whereas in the past, these kinds of high altitude hover trials were challenging since they required high-ground reference points, recent technological developments show potential to make these trials more practical in the future. Matayoshi et al. (Ref. 7) presented results from a flight-test evaluation of a helicopter airborne lidar system. This system can measure accurately three-axis true airspeed which is crucial for high-altitude hover performance trials. Boirun (Ref. 8) attempted to rectify the disadvantage of the conventional hover flight-test method by including compressibility effects into the empirical performance model of the helicopter. However, his approach did not determine a definitive *single* empirical model to include compressibility effects. Instead, various curves for different values of main-rotor tip speeds were presented.

Obtaining an accurate single empirical model to predict the hover performance is highly beneficial since it could also be used for real-time applications. A single empirical hovering model can be used in conjunction with existing algorithms that predict the gross weight of the helicopter for real-time hovering performance. Abraham and Costello (Ref. 9) presented such a practical algorithm to estimate the gross weight and center of mass of a helicopter in flight and reported the algorithm works well in hover.

The authors (Ref. 10,11) presented an alternative and more accurate approach to helicopter performance flight-testing, using multivariable polynomials as empirical models. This approach was proven more accurate (in excess of 300%) in the prediction of the available power of a helicopter under a wide range of atmospheric conditions as compared to the conventional single-variable flight-test method (Ref. 10). Reference 11 provides a systematic method for screening between candidate multivariable predictors. This multivariable polynomial approach is applied to the power required to sustain a helicopter in an OGE hover, without taking any lenient assumptions such as negligible compressibility effects.

An alternative flight-test analysis method to determine the OGE hover performance of a helicopter was derived and is presented herein. After a short introduction, the conventional single-variable method is explained and demonstrated using flight-test data of a Bell Jet-Ranger helicopter. Flight-test data from three sorties totaling 56 data points are used to find an empirical model to estimate the power required to hover OGE. This conventional empirical model is then used to predict 20 hover points, measured on the same helicopter but obtained during a different flight-test sortie. This process is used so that the prediction accuracy of the model can be evaluated. In the third section, an alternative analysis method referred to as the "corrected-variables screening using dimensionality reduction" (CVSDR) is proposed. Starting with fundamental dimensional analysis, a list of 15 corrected variables are generated, which act as the candidate predictors for the OGE hover performance problem. This list of predictors is then refined by executing concepts of dimensionality reduction. The singular-value decomposition (SVD) is exercised to reduce the number of candidate predictors to only four bare-essential and effective corrected variables. The proposed CVSDR method is demonstrated by using the same flight-test data of the Bell Jet-Ranger helicopter. The fourth section compares the different levels of accuracy achieved from the two methods, the conventional and the proposed CVSDR and also provides possible reasoning as to why this difference exists. Finally, conclusions complete the paper.

The Conventional Flight-Test Method for Helicopter Hover Performance

The conventional flight-test method for determining the power a helicopter requires for a hovering flight is based on finding the linear relation between the coefficient of power (C_P) and the coefficient of weight raised to the 1.5 power ($C_w^{1.5}$). This method is thoroughly explained in the literature (Refs. 12–16) and is briefly discussed in this section. Demonstrations of this conventional method are shown in numerous papers, which deal with helicopter hover performance (Refs. 17–20). The main rotor is the primary power consumer in a conventional configuration hovering helicopter (i.e., a helicopter which has a single main rotor and a single tail rotor) since it uses *about* 85% of the total power in an OGE hover. This amount of power directed to the main rotor varies as per different types of helicopters, external configurations, and the different atmospheric conditions.

Since the amount of power delivered to the main rotor is so significant, the mathematical model to represent the hover performance is mainly dictated by the main rotor. This power is comprised of two main terms (Eq. (1)). The first term is referred to as the induced power (or the ideal power) and is derived from the momentum concept. It represents the amount of power required to create the lift (or thrust). The second term in Eq. (1) is referred to as the profile power and is the amount of power required to overcome the viscous effects between the main rotor blades and the surrounding air. The second term was derived using principles of the blade element theory. One should comprehend that Eq. (1) is based on few simplifications such as a uniform distribution of induced velocity across the main-rotor disk, a constant zero-lift drag coefficient (C_{d0}), and a constant chord length of the main-rotor blades.

Next, Eq. (1) is normalized by using the term $(\rho A(\Omega R)^3)$ to yield a nondimensional (ND) equation (Eq. (2)) that uses the coefficient of power (C_P) and coefficient of weight (C_W). The conventional method for hover performance flight-testing is to enforce this main-rotor power theory onto the helicopter as a whole. The flight-tester task is to relate between the measured coefficient of power (C_P) and the coefficient of weight (C_W) under a wide range of gross weights and atmospheric

Table 1. Summary of OGE hover conditions

Sortie	W (lb.)	C_W ($\times 10^{-3}$)	Pressure Altitude (ft)	T_a (°C)	M_{tip}
1	2900–3000	3.298–4.032	2200–6600	11–18	0.59–0.62
2	2850–2960	2.986–4.046	3100–6100	10–15	0.59–0.61
3	2850–2980	3.161–3.739	700–6350	−2 to 3	0.61–0.64
4	2700–3060	3.043–4.062	425–6800	20–26	0.59–0.61

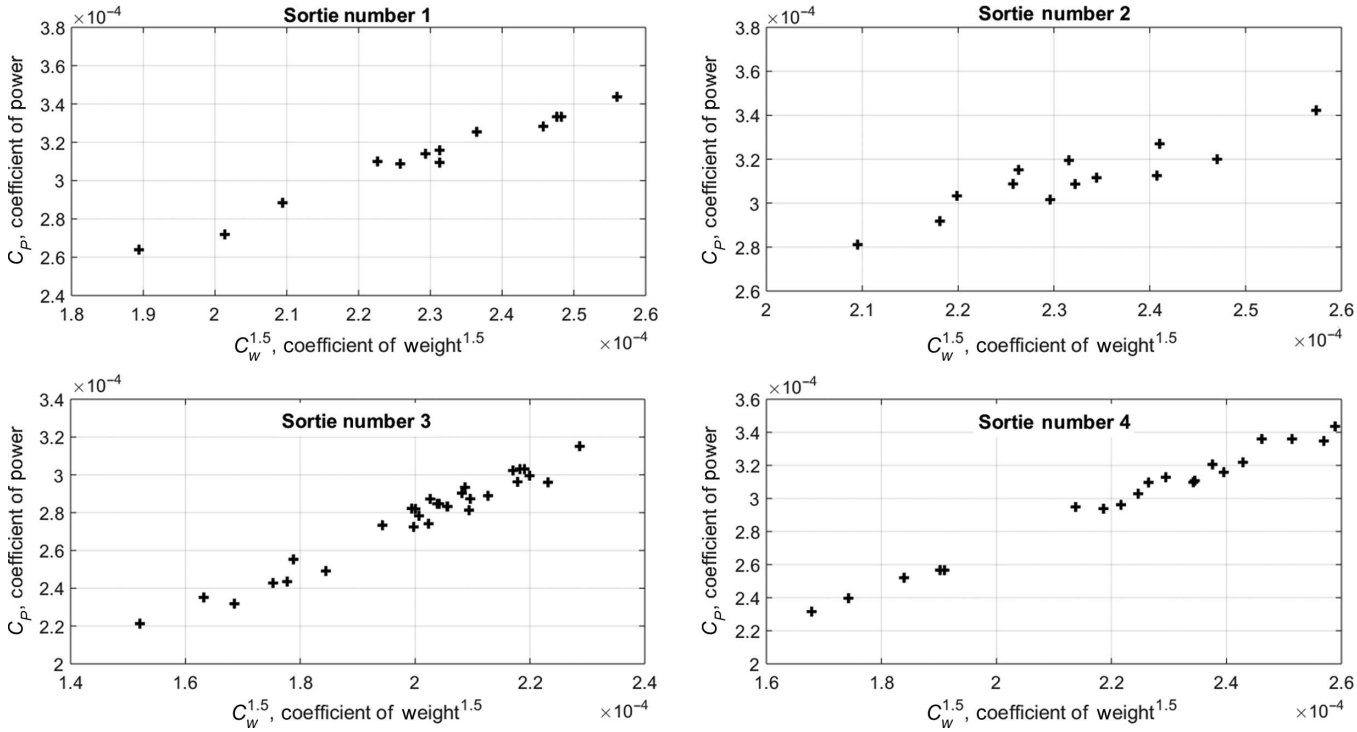

Fig. 1. Nondimensional OGE hover performance of a Bell Jet-Ranger helicopter (four distinct sorties).

conditions. This task is presented mathematically as Eq. (3) for which the flight-tester needs to define the two coefficients (α_1, α_2) for a particular type of helicopter:

$$P_{M/R} = \underbrace{\sqrt{\frac{W^3}{2\rho_a A_d}}}_{\text{(Induced)}} + \underbrace{\frac{1}{8} C_{d_0} \sigma_R \rho_a A_d (\omega R)^3}_{\text{(Profile)}} \tag{1}$$

$$C_{P_{M/R}} = \sqrt{\frac{1}{2}} (C_W)^{1.5} + \frac{1}{8} C_{d_0} \sigma_R \therefore$$
$$C_{P_{M/R}} = \frac{P_{M/R}}{\rho_a A_d (\omega R)^3} \therefore C_W = \frac{W}{\rho_a A_d (\omega R)^2} \tag{2}$$

$$C_P = \alpha_1 (C_W)^{1.5} + \alpha_2 \therefore C_P = \frac{P}{\rho_a A_d (\omega R)^3} \therefore C_W = \frac{W}{\rho_a A_d (\omega R)^2} \tag{3}$$

Next, this conventional method is demonstrated using OGE hovering flight-test data obtained from four distinct sorties of a Bell Jet-Ranger helicopter under different atmospheric and gross-weight conditions, as summarized in Table 1. Figure 1 presents the total of 76 matching pairs of coefficient of power (C_p) and coefficient of weight raised to the 1.5 power ($C_w^{1.5}$) measured in all four sorties. All 76 OGE hover points were obtained using the free-flight (untethered) flight-test technique. Specialty flight-test instrumentation (FTI), which was calibrated for the test, sampled relevant parameters at a rate of 10 cycles per second. The helicopter was stabilized at each hover point for a duration of at least 20 s, and sampled data were averaged over this period of time postflight. The power required to hover was reduced from the engine output torque and the free-turbine speed which were both sampled by the FTI. The gross weight of the helicopter was calculated by subtracting the fuel used from the takeoff all up weight. All hover points were conducted under the restriction of the relative wind to be less than 3 kt. For ground-referenced hover points the wind was measured using a ground-based anemometer and for high altitude hover points, an independent helicopter with an independent low airspeed indicator was used as a hover reference for the tested Jet Ranger.

The level of accuracy achieved using the conventional method was assessed by taking the following approach: flight-test data from the first three sorties were used for the derivation of an empirical OGE hover model, obtained from a linear regression. Then, the accuracy and effectiveness of this empirical model were evaluated by comparing its predictions with the actual flight-test data gathered in Sortie 4. The reason for this specific partition of predicting the performance of Sortie 4 by using data obtained from the first three sorties was to challenge the method to the fullest extent possible. It is evident from Table 1 that Sortie 4 was executed under a wider range of gross weights and pressure altitudes, not covered by the first three sorties. By applying this specific partition, the empirical hovering model is challenged with an extrapolation task.

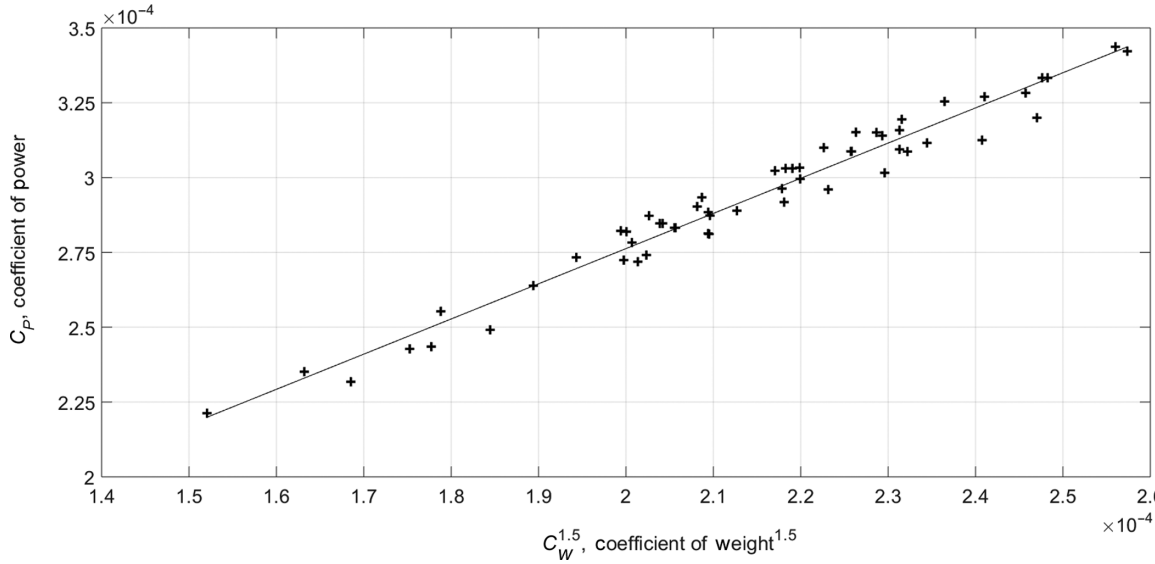

Fig. 2. Nondimensional OGE hover performance of a Bell Jet-Ranger (Sorties 1–3).

Linear regression was executed in order to describe the relationship between the coefficient of power (C_P) and the coefficient of weight raised to the 1.5 power ($C_w^{1.5}$). The 56 flight-test hover points of Sorties 1–3 were substituted in Eq. (3) yielding a linear system of 56 equations with only two unknowns (the coefficients α_1, α_2). This set of equations is compactly represented as Eq. (4):

$$[A]\{\alpha\} = \vec{b} \tag{4}$$

The matrix A is of size (56, 2) and contains the numeral values of the coefficient of weight (C_w) raised to the 1.5 power as the first column and a unity vector as the second column. The column vector α is of a size (2, 1) and contains the linear coefficients (α_1, α_2). The column vector b is of size (56,1) and contains the numerical values of the measured coefficient of power (C_P) for all of the hover points. The explicit representation of Eq. (4) is presented as Eq. (5).

The system of equations represented as Eq. (5) is overdetermined and does not have an exact solution. However, one can look for the "closest" solution of this system, that is, the "best-fit" solution denoted as $\hat{\alpha}$ (Ref. 21). The matrix constructed from $[A^T A]^{-1} A^T$ is defined as the *projection matrix*, and when multiplied by the vector b provides the best-fit solution or the "closest" solution one can look for (Eq. (6)). Although this specific example solves for only two coefficients (α_1, α_2), this method is applicable for an overdetermined system with any arbitrary number of coefficients.

$$\begin{bmatrix} C_{w_1}^{1.5} & 1 \\ C_{w_2}^{1.5} & 1 \\ \cdot & \cdot \\ \cdot & \cdot \\ \cdot & \cdot \\ C_{w_{56}}^{1.5} & 1 \end{bmatrix} \begin{bmatrix} \alpha_1 \\ \alpha_2 \end{bmatrix} = \begin{bmatrix} C_{P_1} \\ C_{P_2} \\ \cdot \\ \cdot \\ \cdot \\ C_{P_{56}} \end{bmatrix} \tag{5}$$

$$\{\hat{\alpha}\} = [A^T A]^{-1} A^T \vec{b} \tag{6}$$

For the example considered in this paper, the regressed OGE hover empirical model of the Bell Jet-Ranger is presented as Eq. (7). Figure 2 presents all 56 data points from the first three sorties and the "best-fit" solution (Eq. (7)). The errors between the measured and the predicted OGE hovering power for Sortie 4 were calculated in accordance with Eq. (8) and are presented in Fig. 3. The prediction errors ranged up to an absolute maximum value of 11.7 hp, a mean of −3.7 hp, and variance of 18.1 hp^2. For the type of helicopter tested, a power deviation of more than 1.6 hp (absolute value) is already clearly evident to the aircrew. The averaged prediction error of −3.7 hp (overestimate) with a variance of 18.1 hp^2 is therefore considered substantial.

The conventional approach in flight-testing for assessing "how accurate" does a model predict the actual performance is based on hypothesis testing. This approach which follows from the central-limit theorem is thoroughly discussed in the literature (Refs. 22, 23). In a nutshell, a hypothesis is set (the "null hypothesis") and by using the test statistic (Eq. (9)) the validity of the null hypothesis is assessed against the alternative hypothesis. For the specific case presented, the null hypothesis assigned is that *on average* the power-to-hover predicted by the empirical model obtained (Eq. (7)) does not differ from the true measured power by more than ±1.6 hp (deviation mismatch noticeable to the Jet-Ranger aircrew). This null hypothesis is tested against the alternative that on average the power to hover from Eq. (7) shows an absolute prediction error of more than 1.6 hp.

$$C_P|_{(S_{1-3})} = 1.175(C_W)^{1.5} + 4.118 \times 10^{-5} \text{ (Base model)} \tag{7}$$

$$\vec{E}_r|_{\text{base}} = \left(C_{p_i} - \left(1.175\left(C_{W_i}\right)^{1.5} + 4.118 \times 10^{-5}\right)\right)\rho_{a_i} A_d(\omega_i R)^3 \;\; \therefore \; i = 1, 2, ..., 20 \tag{8}$$

$$t_{\text{base}} = \frac{|\bar{E}_r|_{\text{base}}| - \mu_0}{S_{\text{base}}/\sqrt{n}} \;\; \therefore \mu_0 = 1.6\,\text{hp} : n = 20 \tag{9}$$

The relevant test statistic for this hypothesis testing is calculated per Eq. (9). The symbol n represents the number of measured test points of Sortie 4 ($n = 20$), and S stands for the standard deviation of the prediction errors of the empirical hover model (Eq. (7)), which are presented in Fig. 3. The calculated value for the test statistic (Eq. (9)) was found to be 2.18. Inferential statistical analysis based on the sampled data from Sortie 4 shows the probability for making a type I error by rejecting the null hypothesis to be only 4.2%. This low probability for a type I error is below the 5% significance level accustomed in helicopter performance flight-testing. The practical meaning of this test is that there is significant

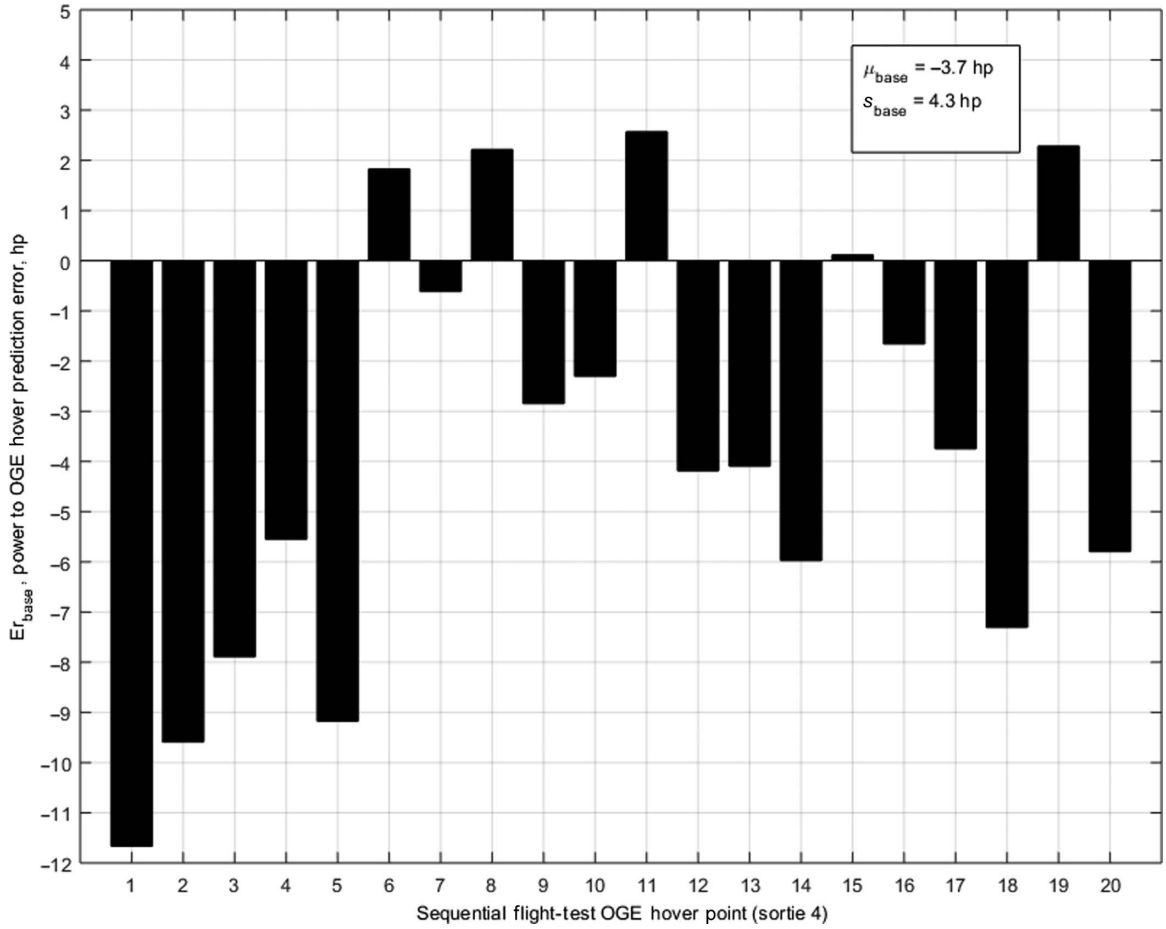

Fig. 3. Power to hover prediction errors for Sortie 4 (base model).

statistical evidence at the 95% confidence level to reject the null hypothesis and adopt the alternative hypothesis instead. It can be concluded that *on average* and at the 95% confidence level, the power required to hover predictions (Eq. (7)) deviates by more than 1.6 hp from the actual measured power. Complementary statistical analysis shows that *on average* and at the 95% confidence level, the hover power predictions based on Eq. (7) deviate by up to 1.7 hp from the actual measured power.

This noticeable prediction error of the conventional hovering model is to be expected. One should doubt the linear relation between the coefficient of power and the coefficient of weight raised to the 1.5 power (C_p, $C_w^{1.5}$). Merely by observing Fig. 2, one should doubt if the relation is actually linear and whether there are some other latent factors that affect the relation between the data points.

Concluding, the conventional flight-test method for assessing the OGE power required to hover can result in substantial estimation errors as demonstrated for the prediction of Sortie 4. Statistical analysis at the 95% confidence level shows that *on average* the hover power predictions based on Eq. (7) deviate by up to 1.7 hp from the actual measured power. In the next section, an alternative analysis method with an improved prediction accuracy is proposed.

Corrected Variables Screening Using Dimensional Reduction Method

An alternative analysis method for the power required to hover is proposed, referred to as the CVSDR. The method requires no variation to the manner flight-test sorties are carried out; only the analysis method is modified. The method involves three phases. In phase one, an original list of corrected variables is generated for a multivariable analysis approach. In phase two, this list of corrected variables is refined based on concepts of dimensionality reduction. Phase three starts once the bare essential list of corrected variables is acquired, and an empirical multivariable model is fitted to the flight-test data. The entire derivation process is demonstrated hereafter using flight-test data from a Bell Jet-Ranger helicopter.

Phase One: Original list of corrected variables to represent hover performance

Beginning by suggesting the dimensional variables that affect the physical problem of the amount of power required to hover a helicopter. These are the ambient static pressure, P_a, the ambient static temperature, T_a, the helicopter gross weight, W, the main-rotor disk area, A_d, the main rotor angular speed, ω, and the main-rotor height above the ground, h. The power required to hover, P, can be represented mathematically as Eq. (10) and Eq. (11) in an implicit form. The dimensions involved are presented in Table 2, where M represents mass, L represents length, and T represents time.

$$P = f(P_a, T_a, W, A_d, \omega, h) \tag{10}$$

$$\hat{f}(P, P_a, T_a, W, A_d, \omega, h) = 0 \tag{11}$$

Table 2. Summary of all variables and dimensions involved

#	Physical Variable	Notation	Dimension
1	Power required to hover	P	$[M][L]^2[T]^{-3}$
2	Ambient static pressure	P_a	$[M][L]^{-1}[T]^{-2}$
3	Ambient static temperature	T_a	$[L]^2[T]^{-2}$
4	Helicopter gross weight	W	$[M][L][T]^{-2}$
5	Main-rotor disk area	A_d	$[L]^2$
6	Main-rotor angular speed	ω	$[T]^{-1}$
7	Main-rotor height above ground	h	$[L]$

The problem has seven variables involved with three dimensions (L, M, T). According to the Buckingham pi theorem (Ref. 24), the complexity of the problem can be reduced from the seven-dimensional variables dependent on only four ND variables. These four ND variables are next defined as products of the dimensional variables. The four ND variables are denoted by π_i. Since there are seven-dimensional variables to construct four ND variables, three-dimensional variables were used as repeating variables in the ND products (π_i). There are 35 different options to choose three variables out of seven for the case where the order does not matter (combinations). This sets a fairly tedious task of screening between 35 different options, defining the best appropriate manner to describe the ND helicopter hover performance. The derivation is demonstrated for only one of the 35 options available. The following example involves setting the main-rotor disk area, the ambient static pressure, and the ambient static temperature as repeating variables. The four ND products are defined in Eq. (12):

$$\left.\begin{aligned}\pi_1 &= (A_d)^a (P_a)^b (T_a)^c (P)\\ \pi_2 &= (A_d)^d (P_a)^e (T_a)^f (W)\\ \pi_3 &= (A_d)^g (P_a)^h (T_a)^i (\omega)\\ \pi_4 &= (A_d)^j (P_a)^k (T_a)^m (h)\end{aligned}\right\} \tag{12}$$

Next, the dimensional analysis procedure requires to replace each of the dimensional variables with its dimensions and to enforce each one of the four π_i parameters to be nondimensional. This process is demonstrated as per Eq. (13). Each one of the π products yields three equations with three unknowns, which are the exponents. Solving for the exponents of π_1 is demonstrated in Eq. (14). The same process is repeated for each one of the other ND variables, π_2, π_3, and π_4:

$$\left.\begin{aligned}[\pi_1] &= [L^2]^a \left[\tfrac{M}{LT^2}\right]^b \left[\tfrac{L^2}{T^2}\right]^c \left[\tfrac{ML^2}{T^3}\right] = M^{b+1} L^{2a-b+2c+2} T^{-2b-2c-3} = M^0 L^0 T^0\\ [\pi_2] &= [L^2]^d \left[\tfrac{M}{LT^2}\right]^e \left[\tfrac{L^2}{T^2}\right]^f \left[\tfrac{ML}{T^2}\right] = M^{e+1} L^{2d-e+2f+1} T^{-2e-2f-2} = M^0 L^0 T^0\\ [\pi_3] &= [L^2]^g \left[\tfrac{M}{LT^2}\right]^h \left[\tfrac{L^2}{T^2}\right]^i \left[\tfrac{1}{T}\right] = M^h L^{2g-h+2i} T^{-2h-2i-1} = M^0 L^0 T^0\\ [\pi_4] &= [L^2]^j \left[\tfrac{M}{LT^2}\right]^k \left[\tfrac{L^2}{T^2}\right]^m [L] = M^k L^{2j-k+2m+1} T^{-2k-2m} = M^0 L^0 T^0\end{aligned}\right\} \tag{13}$$

$$\left.\begin{aligned}&[M] : b + 1 = 0\\ &[L] : 2a - b + 2c + 2 = 0\\ &[T] : -2b - 2c - 3 = 0\end{aligned}\right\} \Rightarrow \begin{bmatrix}0 & 1 & 0\\ 2 & -1 & 2\\ 0 & -2 & -2\end{bmatrix}\begin{Bmatrix}a\\ b\\ c\end{Bmatrix} = \begin{Bmatrix}-1\\ -2\\ 3\end{Bmatrix}$$

$$\Rightarrow \begin{Bmatrix}a\\ b\\ c\end{Bmatrix} = \begin{Bmatrix}-1\\ -1\\ -\frac{1}{2}\end{Bmatrix} \tag{14}$$

Based on Eq. (14), the first ND variable, π_1, can be written as Eq. (15):

$$\pi_1 = \frac{P}{A_d \cdot P_a \sqrt{T_a}} \tag{15}$$

The interest is in developing a method to gather hover performance for a specific helicopter and not in drawing a comparison between different types of helicopters. Therefore, the ND variable (Eq. (15)) can be further simplified. The main-rotor disk area (A_d) is constant, and the static pressure (P_a) and temperature (T_a) of the ambient air can be expressed as per their ratio to the standard sea-level values (Eq. (16)). This gives a simplified expression for π_1 (Eq. (17)) defined as π_1^*. Since this term has dimensions and is not a pure ND, it is better defined as a "corrected" variable to describe the hover performance of a specific helicopter. It can be used to facilitate the forthcoming analysis:

$$P_a = P_0 \cdot \delta \therefore T_a = T_0 \cdot \theta \tag{16}$$

$$\begin{aligned}\pi_1 &= \frac{P}{A_d P_a \sqrt{T_a}} = \frac{P}{A_d P_0 \delta \sqrt{T_0 \theta}} = \frac{P}{\left(A_d P_0 \sqrt{T_0}\right) \delta \sqrt{\theta}}\\ &= \frac{1}{A_d P_0 \sqrt{T_0}} \frac{P}{\delta \sqrt{\theta}} = \text{Const} \cdot \frac{P}{\delta \sqrt{\theta}} \Rightarrow \pi_1^* = \frac{P}{\delta \sqrt{\theta}}\end{aligned} \tag{17}$$

Similar analysis that was performed for π_2, π_3, and π_4 yielded the other three corrected variables (π_2^*, π_3^*, and π_4^*). The hover performance of a specific helicopter can now be simplified as presented as Eq. (18). One should be reminded that π_4 is a true ND variable, which represents the ND height of the main rotor above the ground. This ND variable is beneficial only if the hover performance deals with in-ground-effect. This paper is limited to the OGE only and does not address the ground effect on hover performance.

$$\pi_2^* = \frac{W}{\delta} \therefore \pi_3^* = \frac{\omega}{\sqrt{\theta}} \therefore \pi_4 = \frac{h}{\sqrt{A_d}} \tag{18}$$

Identical dimensional analysis was repeated to evaluate all other 34 possibilities of choosing three-dimensional variables out of the seven. Ten options were found to not have a unique solution, and few other options returned repeated ND variables. Overall, the analysis yielded 15 different corrected variables which can be used for the specific hover performance analysis. Table 3 summarizes all 15 corrected variables in an array form to indicate which of the three-dimensional variables (power, weight, and main-rotor angular speed) is used in the specific corrected variable. Three of the corrected variables (π_{13}^*, π_{14}^*, π_{15}^*) are based on all three-dimensional variables.

Phase Two: Screening for the essential corrected variables using dimensionality reduction

Phase two of the proposed CVSDR method is to refine the list of 15 corrected variables (Table 3) generated from fundamental dimensional analysis and to select only the essentials for the task of acquiring an empirical model to represent the OGE hover performance of a helicopter. A power-based corrected variable needs to be expressed as a function of few other corrected variables. It is immediately evident that the three corrected variables (π_{13}^*, π_{14}^*, π_{15}^*) cannot serve as effective predictors since each one of them simultaneously involves all three major variables of power, weight, and angular speed of the main rotor. Even prior to implementing dimensionality reduction tools, the list of candidate corrected variables is reduced to 12 candidate predictors.

The singular value decomposition theorem. The dimensionality reduction proposed is based on the linear algebra concept known as the SVD. According to this concept, which is thoroughly explained in the literature

Table 3. Corrected Variables to represent the OGE hover performance

	Power Based	Weight Based	Main-Rotor and Angular-Speed Based	Power, Weight, and Main-Rotor Angular Speed Based
Power based	$\pi_1^* = \frac{P}{\delta\sqrt{\theta}}$	$\pi_6^* = \frac{P}{W\sqrt{\theta}}$	$\pi_4^* = \frac{P}{\delta\omega}$	$\pi_{13}^* = \frac{P}{W\omega}$
	$\pi_5^* = \frac{P}{\delta^2\theta}$	$\pi_8^* = \frac{P^4}{W^5\delta}$	$\pi_{10}^* = \frac{P\omega^2\sqrt{\theta^3}}{\delta}$	$\pi_{14}^* = \frac{P\sqrt{\delta}}{\omega\sqrt{W^3}}$
		$\pi_9^* = \frac{P\sqrt{\theta}}{W^2}$	$\pi_{12}^* = \frac{P\omega^2}{\delta\sqrt{\theta^3}}$	$\pi_{15}^* = \frac{P\sqrt{\delta}}{W\omega}$
Weight based		$\pi_2^* = \frac{W}{\delta}$	$\pi_{11}^* = \frac{W\omega^2}{\delta\cdot\theta}$	
Main-rotor angular			$\pi_3^* = \frac{\omega}{\sqrt{\theta}}$	
speed based			$\pi_7^* = \frac{\omega}{\sqrt{\delta}}$	

(Ref. 25), any matrix with real entries can be *uniquely* decomposed into a set of three matrices as given in Eq. (19). Consider a real matrix Z to be of size 'm' by 'n' (notation (m, n)) and rank 'r'. Matrix Z can be expressed as a product of the following three unique matrices:

1) Matrix U called the "left-singular vectors" (LSV) is an orthonormal matrix of size (m, r). The columns of this matrix are unity-norm vectors, which are orthogonal to each other. This set of vectors serves as a basis for the column space of matrix Z.

2) Matrix Σ is a diagonal matrix (size (r, r)) which holds the singular values of Z as entries along its diagonal. The singular values are nonnegative real numbers that can be arranged along the diagonal in descending order.

3) Matrix V called the "right-singular vectors" (RSV) is an orthonormal matrix of size (n, r). The columns of this matrix (or the rows of V^T) are unity-norm vectors, which are orthogonal to each other. The set of these vectors serves as a basis for the row space of matrix Z.

One should consider this decomposition as a way of finding convenient orthogonal bases for both the column space and the row space of an arbitrary real matrix:

$$Z = U\Sigma V^T = \begin{bmatrix} u_{1,1} & u_{1,2} & \cdot & u_{1,r} \\ u_{2,1} & u_{2,2} & \cdot & u_{2,r} \\ \cdot & \cdot & \cdot & \cdot \\ \cdot & \cdot & \cdot & \cdot \\ u_{m,1} & u_{m,2} & \cdot & u_{m,r} \end{bmatrix} \begin{bmatrix} \sigma_1 & & & \\ & \sigma_2 & & \\ & & \cdot & \\ & & & \sigma_r \end{bmatrix} \begin{bmatrix} v_{1,1} & v_{2,1} & \cdot & v_{n,1} \\ v_{1,2} & v_{2,2} & \cdot & v_{n,2} \\ \cdot & \cdot & \cdot & \cdot \\ v_{1,r} & v_{2,r} & \cdot & v_{n,r} \end{bmatrix}$$

$$\sigma_1 > \sigma_2 > \cdots > \sigma_r \geq 0 \tag{19}$$

The SVD of a real matrix can alternatively be regarded as in Eq. (20), which is a combination of r rank-one matrices. This complementary way to look at the SVD is referred to as a spectral decomposition of the matrix Z. With this approach, any real matrix Z of rank r can be approximated as a lower than rank r matrix. This reduction in the rank of the matrix is the essence of the dimensionality reduction of matrix Z:

$$Z = \sigma_1 \begin{bmatrix} u_{1,1} \\ u_{2,1} \\ \cdot \\ \cdot \\ u_{m,1} \end{bmatrix} [\, v_{1,1} \; v_{2,1} \cdot v_{n,1} \,] + \sigma_2 \begin{bmatrix} u_{1,2} \\ u_{2,2} \\ \cdot \\ \cdot \\ u_{m,2} \end{bmatrix} [\, v_{1,2} \; v_{2,2} \cdot v_{n,2} \,]$$

$$+ \cdots + \sigma_r \begin{bmatrix} u_{1,r} \\ u_{2,r} \\ \cdot \\ \cdot \\ u_{m,r} \end{bmatrix} [\, v_{1,r} \; v_{2,r} \cdot v_{n,r} \,]$$

$$\sigma_1 > \sigma_2 > \cdots > \sigma_r \geq 0 \tag{20}$$

SVD implementation for corrected variables screening. The SVD theorem can be implemented for refining the corrected variable list and to identify those which stand out from the group of 12 as the most effective predictors for the OGE hover empirical model. A similar approach was performed in the process of gas-turbine empirical models screening in Ref. (11). For this, matrix Z is filled with numeral entries of the 12 corrected variables as evaluated for the first three flight-test sorties of the Bell Jet-Ranger helicopter. Matrix Z becomes of size (56,12). Each column of the 12 represents a different corrected value (π_1^* to π_{12}^*), and each row represents a distinct single hover point. Next is to normalize the columns of Z to have a mean of zero and a variance of 1. For this, each entry along the column of Z is normalized as per Eq. (21).

Matrix Z is then decomposed into its unique three matrices as per Eq. (19). As expected, the rank of Z is 12 representing the dimensionality of the flight-test data. The OGE hover performance problem as appears in matrix Z can be represented by using all 12 corrected variables (π_1^* to π_{12}^*). However, not all corrected variables have the same level of significance in representing the variance in the flight-test data held by matrix Z. The singular values (σ_i), which are arranged along the main diagonal of matrix Σ in descending order, are key to understanding the level of importance each corrected variable (i) holds. The conceptual interpretation of the SVD of Z for the specific problem of OGE hover performance is illustrated in Fig. 4 and is further explained herein.

The 12 singular values of the diagonal matrix Σ are normalized as per Eq. (22). The normalized singular values are presented in Fig. 5 along with a cumulative-sum plot of all normalized singular values. The main conclusion one can draw from Fig. 5 is that the dimensionality of the general OGE hover problem can be practically reduced from 12 (the general case) to only five for the specific OGE hover analyzed. The empirical model representing the general OGE hover performance can be substantially simplified for the specific case analyzed, to include only five corrected variables, instead of the original 12. The cumulative sum plot presented in Fig. 5 indicates that 98% of the variance in the flight-test data stored in matrix Z can be captured by using only the first five most significant corrected variables. Also from Fig. 5, it can be observed that the most significant dimension of the problem is responsible for 52% of the variance in the flight-test data, the second dimension explains 19% of the variance in the data, and the third, fourth, and fifth can explain 13%, 8%, and 6%, respectively.

The next question one might ask is "which are the most significant corrected variables?" This can be answered by evaluating the absolute values of the entries of the RSV matrix. As illustrated in Fig. 4, each row of the RSV indicates the level of correspondence to a specific singular value or a dimension of the problem. For example, the first row of the RSV specifies the level of correspondence each one of the 12 corrected

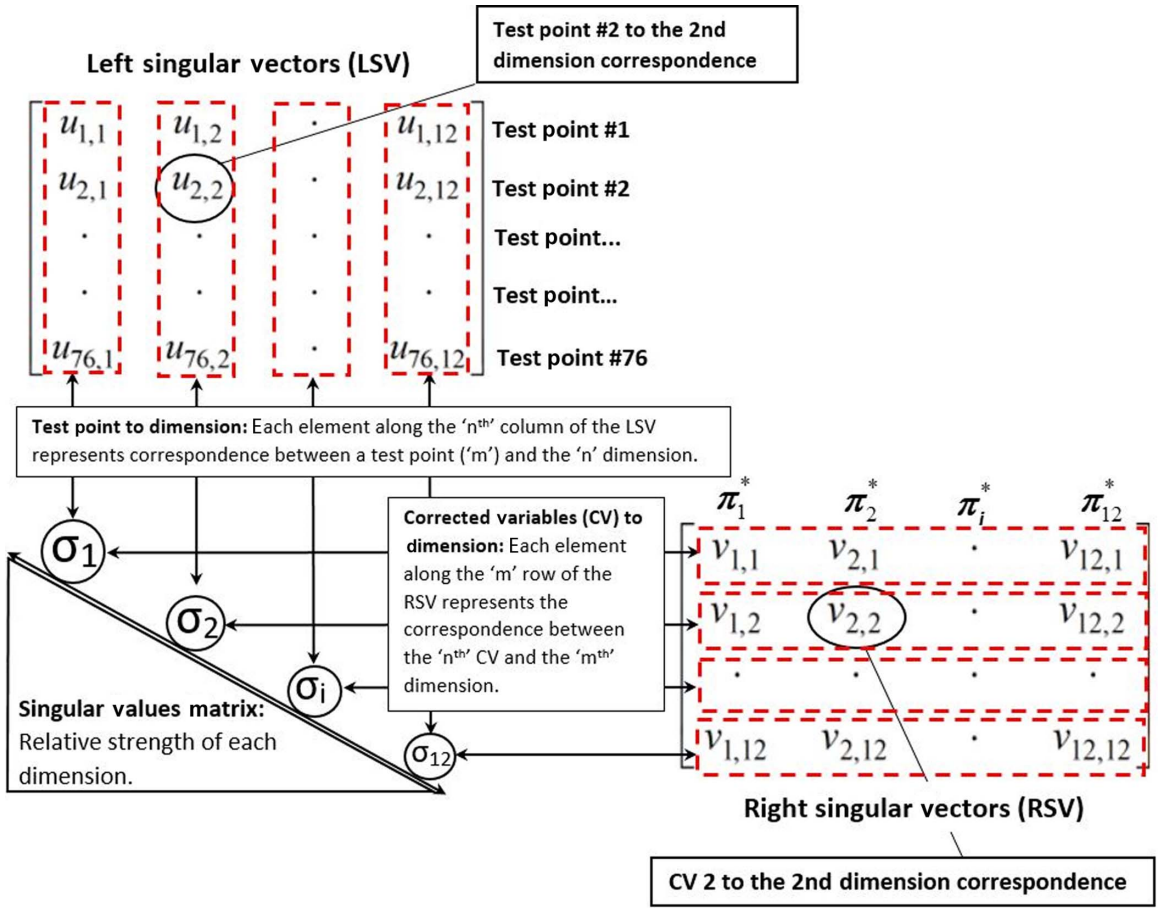

Fig. 4. The conceptual interpretation of the SVD of matrix Z.

variables has to the first (and most significant) singular value. The second row of the RSV indicates the correspondence between all 12 corrected variables to the second most significant dimension of the problem and so on. Since the dimensionality of the problem was reduced from 12 to 5, it is required to evaluate the first five rows of the RSV matrix in order to expose the most significant corrected variables of the OGE hover problem. Figure 6 presents the significance of each corrected variable to each one of the five substantial dimensions of the OGE hover performance problem by indicating the normalized values (as per Eq. (23)) of the entries along the first five rows of the RSV matrix.

The LSV matrix has no major role in the type of analysis addressed in this paper since it only indicates the level of correspondence between each one of the 56 OGE hover points and the singular values of Z. This type of correspondence between particular hover test points and the various dimensions of the OGE hover performance was deemed irrelevant to the topic analyzed.

The following conclusions are drawn from Figs. 5 and 6: (1) the first and most significant dimension of the OGE hover problem, which holds for 52% of the variance in the data, is best represented by π^*_{12}. (2) The second most significant dimension of the OGE hover problem, which holds for 19% of the variance in the data, is best represented by π^*_{11}. (3) The third dimension of the OGE hover problem, which holds for 13% of the variance in the data, is best described by π^*_2. (4) The fourth dimension of the problem, which holds for 8% of the variance in the data, is best represented by π^*_{12}. (5) The least significant dimension in the truncated list of five dimensions holds for only 6% of the variance in the data and is best represented by π^*_9, followed by π^*_7. Since only one power-based predictor is required for the empirical model in the quest and the previous conclusions suggest two (π^*_{12} and π^*_9), it was decided to use the one that shows the highest correspondence with the first dimension which is π^*_{12}. Furthermore, π^*_9 was replaced with π^*_7 as the predictor which best represents the fifth dimension of the OGE hover problem.

Finally, a conceptual empirical model to represent the OGE hover performance of the example helicopter can be stated as Eq. (24). This conceptual relationship is next pursued with a first-order linear model as described in Eq. (25).

The multiple steps performed for dimensionality reduction in phase two are presented as a flow chart in Fig. 7 for further simplification:

$$\pi'_i = \frac{\pi^*_i - \mu_{\pi^*_i}}{S_{\pi^*_i}}, i = 1, 2, ..., 11, 12 \tag{21}$$

$$\hat{\sigma}_i = \frac{\sigma_i}{\sum_{k=1}^{12} \sigma_k}, i = 1, 2, 3, ..., 11, 12 \tag{22}$$

$$\hat{V}(i, j) = \frac{|V(i, j)|}{\sum_{j=1}^{12} |V(i, j)|}, i = 1, 2, 3, 4, 5 \tag{23}$$

$$\pi^*_{12} = f_1(\pi^*_{11}, \pi^*_2, \pi^*_7) \therefore \frac{P\omega^2}{\delta\sqrt{\theta^3}} = f_1\left(\frac{W\omega^2}{\delta \cdot \theta}, \frac{W}{\delta}, \frac{\omega}{\sqrt{\delta}}\right) \tag{24}$$

$$\frac{P\omega^2}{\delta\sqrt{\theta^3}} = \beta_1\left(\frac{W\omega^2}{\delta \cdot \theta}\right) + \beta_2\left(\frac{W}{\delta}\right) + \beta_3\left(\frac{\omega}{\sqrt{\delta}}\right) + \beta_4 \tag{25}$$

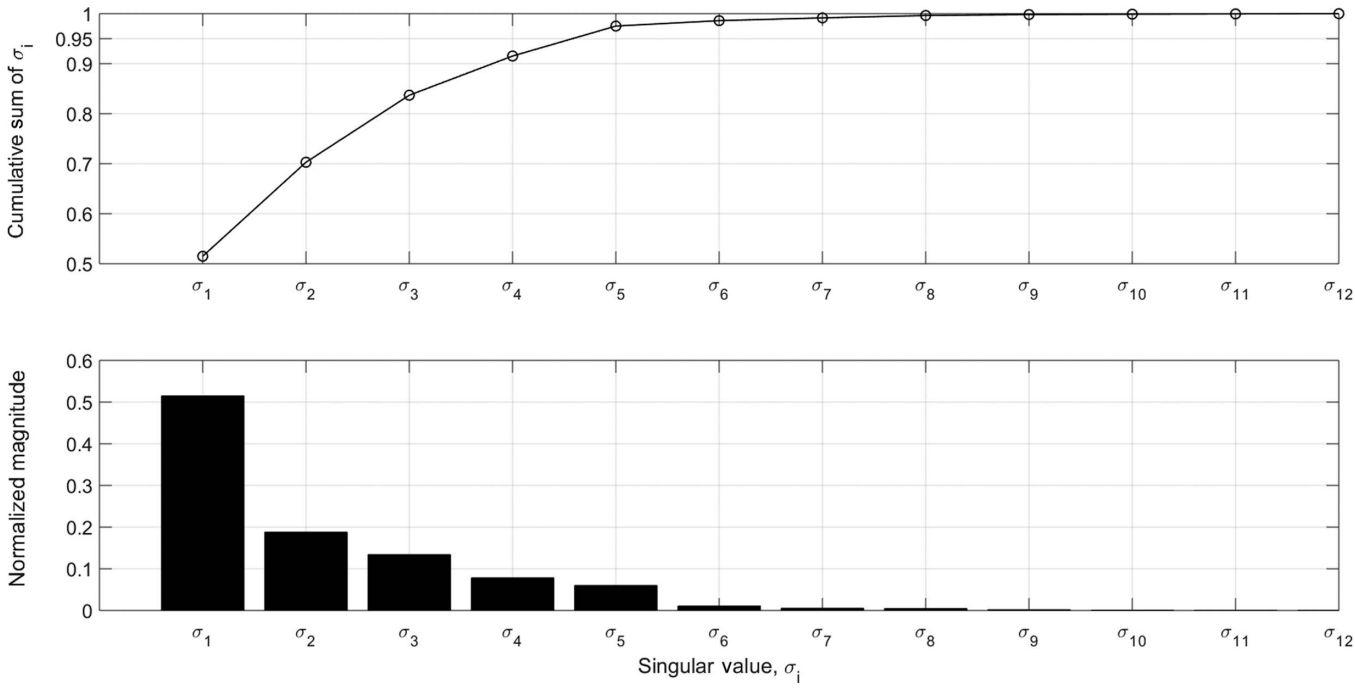

Fig. 5. The singular values of matrix Z (hover performance dimensions).

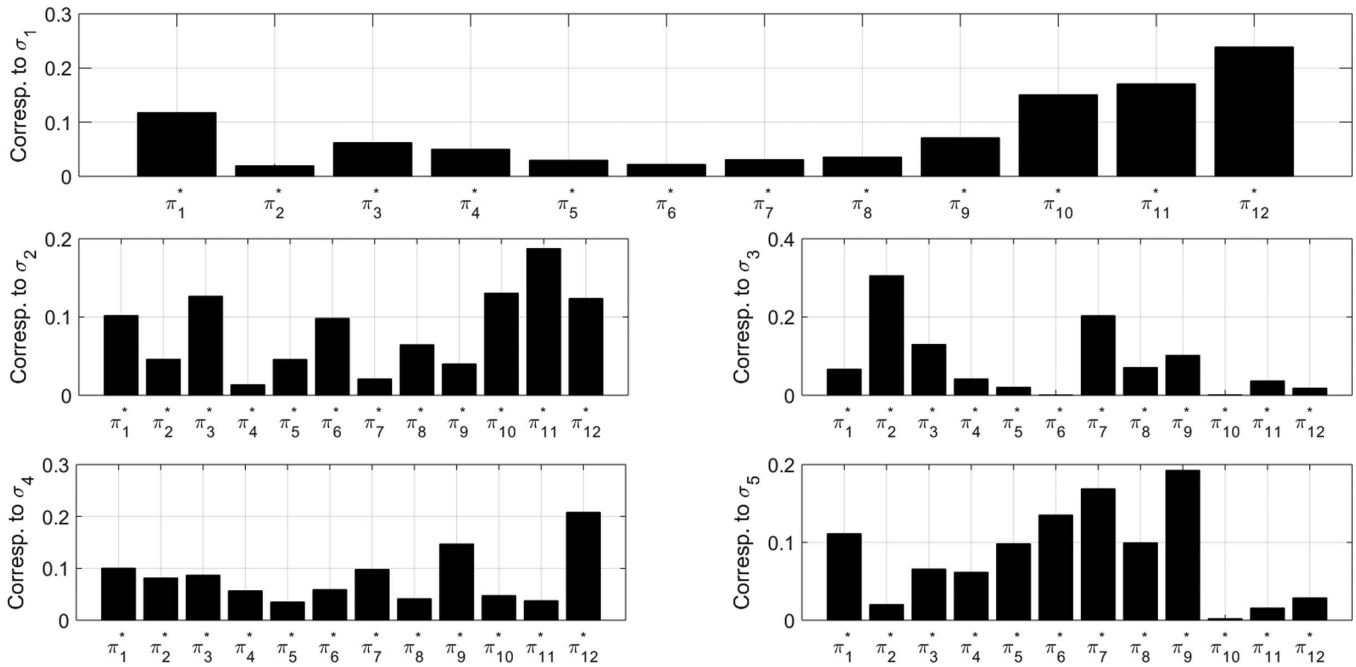

Fig. 6. Correspondence between corrected variables and the hover performance dimensions.

Phase Three: Deriving a practical empirical model

The proposed model (Eq. (25)) was fitted with the 56 flight-test OGE hover points from the first three sorties. This regression process was based on the "least-squares" method as previously explained in the second section. The refined OGE hover model, based on the CVSDR method and the flight-test data from the first three sorties, is presented as Eq. (26). This empirical model is addressed hereinafter as Model number 1 and denoted as M1.

Next is to use this refined OGE hover Model 1 (Eq. (26)) in order to predict the power required to OGE hover for the conditions of Sortie 4. The errors between the predicted power and the actual measured power were calculated in accordance with Eq. (27) and are presented in Fig. 8. Prediction errors ranged up to a maximum absolute deviation of 8.5 hp. The mean of the prediction errors for the 20 hover points of Sortie 4 was calculated to be -2.3 hp with a variance of 9.7 hp^2.

Similar statistical analysis as explained in the second section for the base model was performed in order to evaluate the level of accuracy to

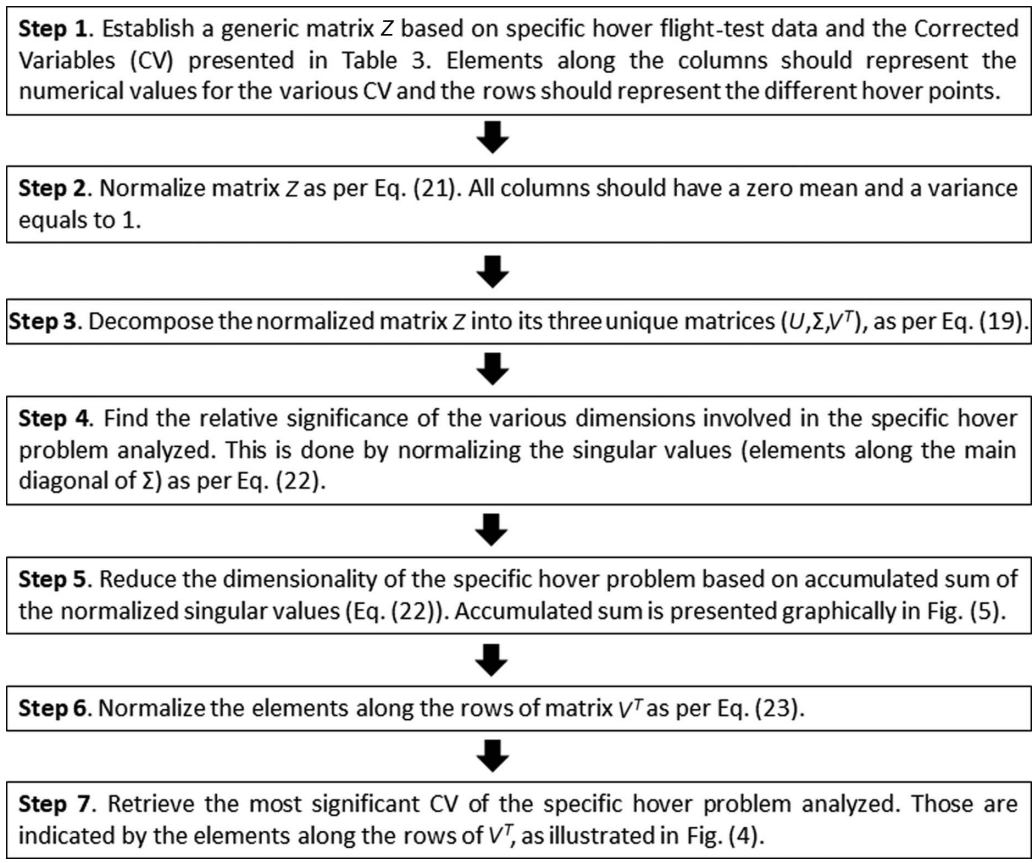

Fig. 7. Steps required for dimensionality reduction in phase two.

be expected from the refined OGE hover model (Model 1). The applicable test statistics for the relevant hypothesis testing were calculated per Eq. (28). The symbol n represents the number of measured test points of Sortie 4 ($n = 20$) and S_{M1} stands for the standard deviation of the prediction errors of Model 1 (the standard deviation of the data presented in Fig. 8. The test statistic was found to be 1.06. Inferential statistical analysis based on the sampled data from Sortie 4 shows a significant probability of 30.1% for making a type-I error by rejecting the null hypothesis. This probability for a type-I error is well above the 5% significance level accustomed in helicopter performance flight-testing. Practically, there is no significant statistical evidence at the 95% confidence level to reject the null hypothesis; therefore, it has to be accepted. Complimentary statistical analysis shows that at the 95% confidence-level Model 1 (Eq. (26)) predictions deviate *on average* by up to 0.9 hp from the actual measured power to hover. This value of 0.9 hp is well below the deviation threshold of 1.6 hp noticeable to the Bell Jet-Ranger aircrew.

$$\frac{P\omega^2}{\delta\sqrt{\theta^3}} = \beta_1\left(\frac{W\omega^2}{\delta\cdot\theta}\right) + \beta_2\left(\frac{W}{\delta}\right) + \beta_3\left(\frac{\omega}{\sqrt{\delta}}\right) + \beta_4,$$
$$\begin{Bmatrix}\beta_1\\ \beta_2\\ \beta_3\\ \beta_4\end{Bmatrix} = \begin{Bmatrix}0.134\\ -7.99\\ 926.5\\ -2\times 10^5\end{Bmatrix} \text{ (Model 1)} \tag{26}$$

$$\vec{E}_{r_{M1}} = P_i - \left(\beta_1\left(\frac{W\omega^2}{\delta\cdot\theta}\right)_i + \beta_2\left(\frac{W}{\delta}\right)_i + \beta_3\left(\frac{\omega}{\sqrt{\delta}}\right)_i + \beta_4\right)\frac{\delta_i\sqrt{\theta_i^3}}{\omega_i^2}, i = 1, 2, ..., 20 \tag{27}$$

$$t_{M1} = \frac{\left|\bar{E}_{r_{M1}}\right| - \mu_0}{S_{M1}/\sqrt{n}}, \mu_0 = 1.6 \text{ hp}, n = 20 \tag{28}$$

Proposed CVSDR and Conventional Methods Comparison

As previously noted, the OGE hover flight-test data obtained using a Bell-Jet Ranger helicopter in a course of four different sorties were divided into two groups. The first, which consisted of data from the first three sorties, was used to develop an empirical model to represent the power for OGE hover. This model was evaluated for accuracy while used to predict hover points of Sortie 4. Two different models were used, the base model, which relies on the conventional hover flight-testing method (the C_P to $C_w^{1.5}$ method), and another original multivariable empirical model, which is based on the proposed CVSDR method. The proposed multivariable empirical model was based on three corrected variables or predictors ($\frac{W\omega^2}{\delta\cdot\theta}$, $\frac{W}{\delta}$, $\frac{\omega}{\sqrt{\delta}}$), proposed by the CVSDR method. Figure 9 presents a comparison between the prediction errors of the two OGE hover models: the conventional method (Eq. (7)) and the proposed multivariable Model 1 (Eq. (26)).

The conventional model predicts the hover points of Sortie 4 with an average error of –3.7 hp and variance of 18.1 hp^2. The proposed Model 1 yielded better predictions with an average error of –2.3 hp and a smaller variance of 9.7 hp^2. Hypothesis testing aimed at projecting from the particular case of Sortie 4 to the general case shows that at the accustomed 95% confidence level Model 1 predictions deviate *on average* by only 0.9 hp. Power predictions of the conventional model deviate, on average, by a significant 1.7 hp, which is noticeable to the Jet-Ranger helicopter aircrew. This power deviation of 1.7 hp can be translated to a gross weight

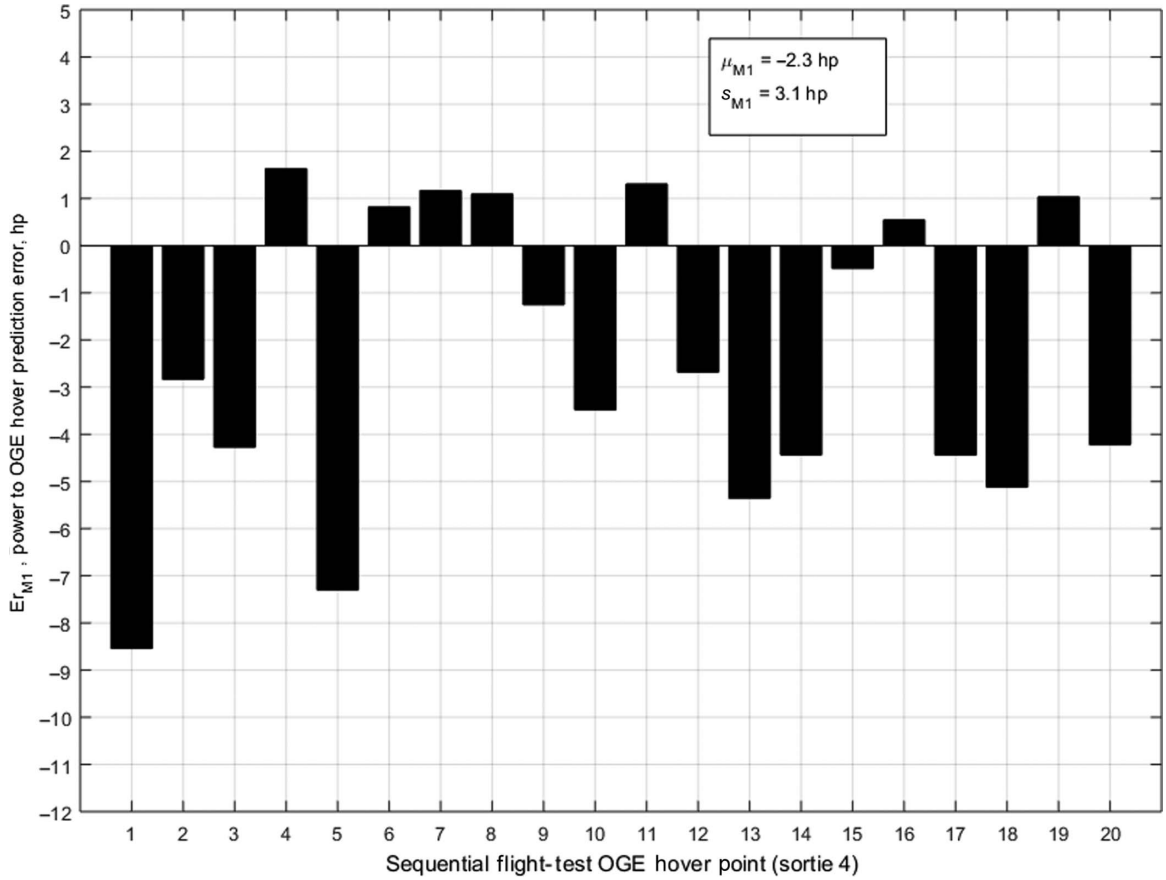

Fig. 8. Power to OGE hover prediction errors of Model 1 (Sortie 4).

difference of about 15 lb under the conditions tested (Sorties 1–4). The power to hover prediction of the proposed CVSDR method was found to be substantially more accurate than the conventional method as its deviation from the actual power was 1.9 times *less* than the conventional method.

One might question why is it that Model 1 predicts the hover power much better than the conventional model? First and foremost, the CVSDR method does not assume beforehand which predictors should be used in the empirical model. Instead, the list of the potential 15 predictors is reduced to the most essential and effective ones based on the *specific* flight-test data analyzed. This approach by itself provides more flexibility which allows for more accurate modeling. Specifically and as emphasized in the introduction, compressibility effects have a substantial influence on the hover performance of rotors as reported by the current CFD analysis. The conventional model neglects compressibility and drag-divergence effects, whereas the multivariable Model 1 employs a predictor to represent the blade tip Mach-number ($\pi_{11}^* = \frac{W\omega^2}{\delta \cdot \theta}$), therefore capable of including compressibility and drag-divergence effects. The inherent assumption of the conventional OGE hover flight-test method for a constant zero-lift drag coefficient (C_{d0}) cannot be held valid for a wide range of Mach numbers and high values of main rotor disk loading. Hovering at low ambient temperatures (high Mach tip numbers) and high gross weights might be responsible for some sections of the main rotor disk to be under drag-divergence conditions. The two predictors (π_7^*, π_{11}^*) used in Model 1 can provide the extra degree of freedom in modeling compressibility effects, which are absent in the conventional model (the C_P to $C_w^{1.5}$ method).

Conclusions

The proposed CVSDR hover performance flight-testing method requires no modification to the manner helicopter hover performance flight-test sorties are carried out. The change is to the procedure of the data analysis. An original list of 15 corrected variables (predictors) to represent the general hover performance of a helicopter was formulated by means of dimensional analysis. This list was further reduced to include only four essential corrected variables by applying concepts of dimensionality reduction on a specific flight-test data measured on a Bell-Jet Ranger helicopter. Using those four essential corrected variables, which represented 98% of the variance in the specific hover performance data, an empirical hover performance model of the helicopter was derived.

The CVSDR method showed great potential as it was used successfully with hover flight-test data of a Bell-Jet Ranger helicopter. The power predictions of the proposed CVSDR method were compared to those of the conventional method and were found to be 1.9 times more accurate. At the 95% confidence level, the CVSDR method deviated by an average of only 0.9 hp from the actual power to hover, whereas the conventional method deviated by an average of 1.7 hp.

Although demonstrated in this paper using flight-test data of a Bell Jet-Ranger helicopter, the CVSDR method is applicable and can be used for OGE hover flight-testing of any other types of conventional helicopters, which employ a single main rotor and a single tail rotor.

The CVSDR method, at its core, is using dimensionality reduction concepts to screen out the most effective and essential predictors of any physically meaningful problem. This capability of the CVSDR method

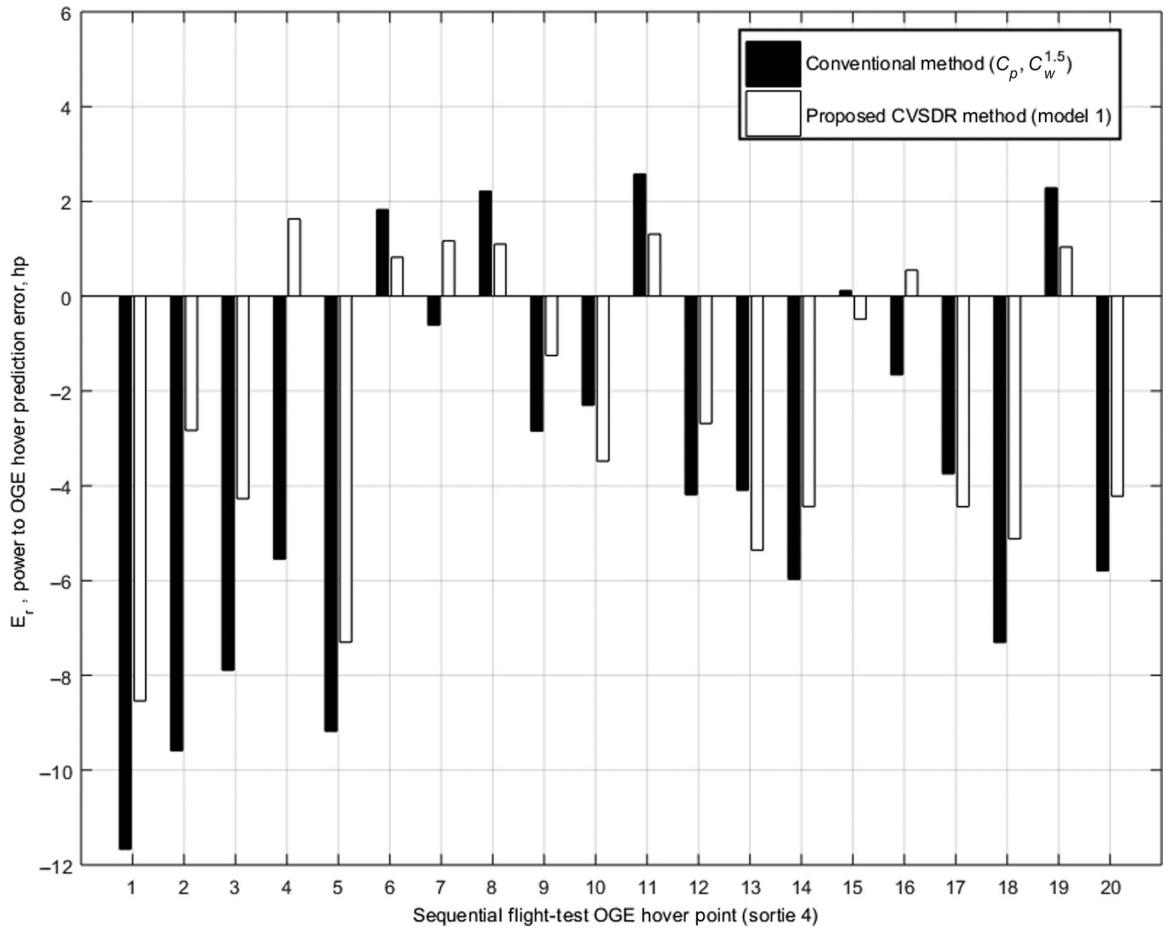

Fig. 9. The conventional and CVSDR methods comparison (Sortie 4 predictions).

can also be applied to other types of helicopter performance flight-testing, which seek to relate ND variables such as level-flight performance.

Future research will include further evaluation of the CVSDR method using hover performance of other helicopter types along with focusing on the suitability and efficiency of employing the CVSDR method to analyze helicopter level-flight performance flight-testing.

References

[1]Leishman, J. G., *Principles of Helicopter Aerodynamics*, 2nd ed., Cambridge University Press, New York, NY, 2006, Chapter 1.

[2]Gessow A., and Myers G., *Aerodynamics of the Helicopter*, 3rd printing, Frederick Ungar Publishing Company, New York, NY, 1967, Chapter 1.

[3]Bousman, W. G., "Out-of-Ground Effect Hover Performance of the UH-60A," UH-60A Airloads Program Occasional Note 2001-01, U.S. Army Aeroflightdynamics Directorate (AMCOM) Ames Research Center, February 2001.

[4]Siva, C., Murugan, M. S., and Ganguli, R., "Uncertainty Qualification in Helicopter Performance Using Monte Carlo Simulations," *Journal of Aircraft*, Vol. 48, (5), 2011, pp. 1503–1511, DOI: 10.2514/1.C000288.

[5]Jacobson, K. E., and Smith, M. J., "Carefree Hybrid Methodology for Rotor Hover Performance Analysis," *Journal of Aircraft*, Vol. 55, (1), 2018, pp. 52–65, DOI: 10.2514/1.C034112.

[6]Garcia, A. J., and Barakos, G. N., "Accurate Predictions of Rotor Hover Performance at Low and High Disc Loadings," *Journal of Aircraft*, Vol. 55, (1), 2018, pp. 89–110, DOI: 10.2514/1.C034144.

[7]Matayoshi, N., Asaka, K., and Okuno, Y., "Flight-Test Evaluation of a Helicopter Airborne Lidar," *Journal of Aircraft*, Vol. 44, (5), 2007, pp. 1712–1720, DOI: 10.2514/1.28338.

[8]Boirun, B. H., "Generalizing Helicopter Flight Test Performance Data (GENFLT)," Proceedings of the 34th Annual National Forum of the American Helicopter Society, Washington, DC, May 15–17, 1978.

[9]Abraham, M., and Costello, M., "In-Flight Estimation of Helicopter Gross Weight and Mass Center Location," *Journal of Aircraft*, Vol. 46, (3), 2009, pp. 1042–1049, DOI: 10.2514/1.41018.

[10]Arush, I., and Pavel, M. D., "Helicopter Gas Turbine Engine Performance Analysis: A Multivariable Approach," *Proceedings of the Institute of Mechanical Engineers, Part G: Journal of Aerospace Engineering*, Vol. 223, (3), 2019, pp. 837–850, DOI: 10.1177/0954410017741329.

[11]Arush, I., Pavel, M. D., and Mulder, M., "A Singular Values Approach in Helicopter Gas Turbine Engine Flight Testing Analysis," *Proceedings of the Institute of Mechanical Engineers, Part G: Journal of Aerospace Engineering*, Vol. 234, (12), 2020, pp. 1851–1865, DOI: 10.1177/0954410020920060.

[12]Leishman, J. G., *Principles of Helicopter Aerodynamics*, 2nd ed., Cambridge University Press, New York, NY, 2006, pp. 212–217.

[13]Prouty, R. W., *Helicopter Performance Stability and Control*, Krieger Publishing Company, Malabar, FL, 1989, Chapter 4.

[14]Knowles, P., "The Application of Non-dimensional Methods to the Planning of Helicopter Performance Flight Trials and Analysis Results," Aeronautical Research Council ARC CP 927, 1967.

[15]Cooke, A. K., and Fitzpatrick E. W. H., *Helicopter Test and Evaluation*, 1st ed., AIAA Education Series, AIAA, Reston, VA, 2002.

[16]National Test Pilot School, *Professional Course Textbook Series, Vol. VII, Rotary Wing Performance Flight Testing*, National Test Pilot School, Mojave, CS, 2017, Chapter 5.

[17]Nagata, J. I., Piotrowski J. L., Young C. J., *et al.*, "Baseline Performance Verification of the 12th Year Production UH-60A Black Hawk Helicopter." Final Report, U.S. Army Aviation Engineering Flight Activity, Edwards AFB, CA, January 1989.

[18]Scmitz S., Bhagwat M., Moulton M. A., *et al.* "The Prediction and Validation of Hover Performance and Detailed Blade Loads," *Journal of the American Helicopter Society*, **54**, 032004 (2009).

[19]Wang, Q., and Zhao Q., "Rotor Aerodynamic Shape Design for Improving Performance of an Unmanned Helicopter," *Aerospace Science and Technology*, Vol. 87, 2019, pp. 478-487, DOI: 10.1016/j.ast.2019.03.006.

[20]Peterson, R. L., and Warmbrodt, W., "Hover Performance and Dynamics of a Full-Scale Hingeless Rotor," Proceedings of the 10th Annual European Rotorcraft Forum, The Hague, The Netherlands, August 28–31, 1984.

[21]Strang, G., *Introduction to Linear Algebra*, 5th ed., Wellesley-Cambridge Press, Wellesley, MA, 2016, Chapter 4.

[22]Guttman, I., Wilks, S., and Hunter, J., *Introductory Engineering Statistics*, 2nd ed., John Wiley & Sons, Inc., New York, NY, 1971, Chapter 10.

[23]Kreyszig, E. *Advanced Engineering Mathematics*, 3rd ed., John Wiley & Sons, Inc., New York, NY, 1972, Chapter 19.

[24]Buckingham, E., "On Physically Similar Systems; Illustrations of the Use of Dimensional Equations," *Physical Review*, Vol. IV, (4), 1914, pp. 345–376, DOI: 10.1103/PhysRev.4.345.

[25]Strang, G., *Introduction to Linear Algebra*, 4th ed., Thomson Brooks/Cole, Belmont, CA, 2006, Chapter 6.